RSC Advances

ROYAL SOCIETY OF CHEMISTRY

www.rsc.org/advances

The stability of B_6 octahedron in BaB_6 under high pressure

Xin Li, Xiaoli Huang, Defang Duan, Gang Wu, Mingkun Liu, Quan Zhuang, Shuli Wei, Yanping Huang, Fangfei Li, Qiang Zhou, Bingbing Liu and Tian Cui*

State key laboratory of Superhard Materials, College of Physics, Jilin University, Changchun 130012, People's Republic of China. E-mail: cuitian@jlu.edu.cn; Fax: +86-431-85168825; Tel: +86-431-85168825

Abstract

We have performed in situ synchrotron X-ray diffraction and first-principles calculations to explore the compressive behaviors of Barium hexaboride (BaB_6) under high pressure. No phase transitions in our experiment are observed up to 49.3 GPa at ambient temperature. It is found that the ambient cage structure (*Pm*-3*m*) is still stable with basic covalent - network during the experimental pressure run. Our theoretical calculations results show that the ambient structure might transform into three dynamically stable structures (*Cmmm*, *Cmcm*, *I*4/*mmm*) at 78 GPa, 97 GPa and 105 GPa respectively. The energy band calculations indicate that the sample is still semiconductor with narrow gap at 50 GPa.

Introduction

The hexaborides MB_6 (M = Y, La, Ca…) have a typical cage structure (*Pm*-3*m*). Owning to non-oxide structure, they have some excellent advantages such as high melting point, high chemical stability, high hardness, low density, and low coefficient of thermal expansion.[1-4] There are also some attractive properties in their various physical phenomena in recent decades. For example, rare-earth hexaborides exhibit Kondo behavior and valence-fluctuations in CeB_6[5]; LaB_6 has low volatility and low work functions through enhancing thermionic emission at high temperature[6]; High superconducting critical temperature (T_c) is found to be 7 K in YB_6[7] and narrow-gap semiconducting behavior exists in YbB_6.[8] Moreover, alkaline-earth metal hexaborides

also have a fascinating feature in magnetism. There is coexistence phenomenon of weak ferromagnetism and antiferroelectricity in boron-deficient MgB_6.[9] Possibly because of a low-density free-electron gas, CaB_6 exhibits weak ferromagnetism in high temperature[10] and then subsequent experiments performed on undoped systems of CaB_6, SrB_6 and La-doped BaB_6 indicating that magnetism might be an intrinsic property of alkaline-earth metal hexaborides,[10-12] whose mechanism might be excitonic insulator by bound electron-hole pairs (excitons) condensing. Hexaborides of Alkaline-earth metal are simple polar semiconductors or semimetal with a fraction of an eV band gap because B_6 molecule acquires two electrons from alkaline-earth metal to form a large divalent B_6 anion and a stable metallic cation. A large number of theoretical calculations and experiments are extensively undertaken and an accredited conclusion is established that the electronic structure of CaB_6 is either semimetal or semiconductor.[10, 11, 13-18] At ambient conditions, MB_6 (M = Ca, Sr, Ba) have a highly symmetrical CsCl-type structure with *Pm*-3*m* space group in which B_6 molecule has the octahedral structure. Metal atoms and B_6 molecules replace the position of Cs and Cl atoms respectively. Recently, Kolmogorov *et al* have found a new structure (*I*4/*mmm*) of CaB_6 under high pressure.[19]

Nevertheless, Barium hexaboride, as an important Alkaline-earth metal hexaboride, is only researched on preparation and properties at ambient conditions.[20] Over the last several years, considerable experimental and theoretical investigations on the electronic band structures and ferromagnetism of alkaline-earth hexaborides have been performed.[21-26] From the results of D. C. magnetization measurements on single crystalline BaB_6, the saturation magnetization at low temperatures is 8 times, in line with other weak ferromagnet of the hexaboride series.[27]

Up to now, research on barium hexaboride under extreme conditions has not been reported. In this article, in order to explore properties of BaB_6 under high pressure, we have carried out in situ synchrotron angle dispersive X-ray diffraction (ADXRD) measurements and first-principles calculations.

Experimental and theoretical methods

BaB_6 powder with a purity of 99.5% was purchased from Alfa Aesar. The sample was ground finely before loaded into the sample chamber. A symmetric diamond anvil cell (DAC) with 300 μm flat culets was used to generate pressure. A tungsten gasket was drilled a 100 um diameter hole in the center as a chamber, which had been precompressed to a thickness of 70 μm. Pressure inside the chamber was determined by the standard ruby fluorescence method.[28] Furthermore, mixture of methanol-ethanol-water (16:3:1, MEW) was selected as the pressure transmitting medium (PTM).[29] In situ ADXRD measurements were carried out at the 4W2 High-Pressure Station of Beijing Synchrotron Radiation Facility (BSRF). The beam size was about 32(H) × 12(V) μm^2 and the incident wavelength was 0.6199 Å. A MAR3450 image plate detector was used to collect the diffraction patterns and the two-dimensional XRD images were radially integrated using the FIT2D software,[30] yielding intensity versus diffraction angle 2θ patterns. Prior to measurement, CeO_2 standard was used to calibrate the geometric parameters. The average acquisition time for each diffraction pattern to obtain sufficient intensity was 300 s. The fitted XRD patterns were completed by means of the Reflex module in the Material Studio Program.[31]

The first-principles calculations were performed with the pseudopotential plane-wave method based on density functional theory (DFT) implemented in the CASTEP[32] and VASP code.[33] The generalized gradient approximation (GGA) with the Perdew−Burke−Ernzerhof (PBE) exchange−correlation functional[34] was used in the calculation of optimizations. The hybrid functional of Heyd, Scuseria and Ernzerhof (HSE06)[35, 36] was also used to verify the results of band structures. A plane-wave cutoff energy of 540 eV was employed for norm-conserving pseudopotentials and the Brillouin zone sampling grids of spacing $2\pi \times 0.03$ $Å^{-1}$. The project-augmented wave (PAW)[37] method was adopted with valence electrons of $2s^2 2p^1$ and $5s^2 5p^6 6s^2$ for B and Ba atoms, respectively.

Results and discussion

Like most of other hexaborides, BaB_6 has a simple cubic crystal structure with

Pm-3*m* space group under ambient conditions. In this structure, six boron atoms form an octahedron connected by covalent bonds and each octahedron connects with six closest octahedrons by covalent bonds that forms a three-dimensional network. Due to this strong covalent network, the framework of *Pm*-3*m* structure is very stable. The schematic representation of BaB_6 crystal structure is shown in Fig. 1(a) and the electron localization function (ELF) of BaB_6 is plotted in Fig. 1 (b) and (c). B_6 octahedron pillages two electrons from Ba atom, and forms a stable divalent B_6 anion. Ba cation inserts interstices of eight B_6 octahedrons, which forms a typical cage structure. There are only two parameters to restrain BaB_6 crystal structure, one is lattice constant a, and another is fractional coordinates (Wyckoff site) of boron atom 6*f* (0.5, 0.5, z). The synchrotron XRD patterns have been obtained from 0.8 GPa to 49.3 GPa using MEW as the PTM. The refinement of BaB_6 has been carried out on an XRD pattern obtained at 0.8 GPa in Fig. 2(a). The refined lattice constant is a = 4.2614 Å and Wyckoff site of B atom is (0.5, 0.5, 0.2053) with unit cell volume V = 77.38 $Å^3$. Selected XRD diffraction patterns from this experimental run are illustrated in Fig. 3(a). It shows that there was no appearance of new peaks when the sample was compressed smoothly up to the highest pressure. In the process of compression, all Bragg diffraction peaks gradually broadened comparing with the initial sharp peaks and shifted toward higher 2θ angles, which indicates that the interplanar distance of crystal planes decreased. The original XRD peaks existed up to the highest pressure 49.3 GPa without appearance of new peaks indicating no occurrence of the phase transition. It confirms the stability of *Pm*-3*m* structure up to 49.3 GPa at least. Besides that, intensity of diffraction peaks were affected by preferred crystallite orientation. Compared with crystallite size, the X-ray beam size was relatively bigger, which could partly reduce mismatch in intensity caused by statistics of measurement.

In order to analyze the evolution of the lattice constants and unit cell volume with pressure, all XRD patterns were refined by Rietveld full profile structure. Fig. 3(b) shows the lattice constant a, B-B_{intra} bond and B-B_{inter} bond length as a function of pressure. The data were linearly fitted without any jumps: k_a = 0.0066 Å•GPa^{-1}, k_{intra}

= 0.00274 Å•GPa^{-1}, k_{inter} = 0.00270 Å•GPa^{-1}. The lattice parameter shows the monotonically decrease with the increasing pressure indicating the reservation of the basic covalent network. We have presented the volume reduction as a function of pressure in Fig. 4. The experimental pressure-volume data were fitted by third-order Birch-Murnaghan (BM) equation of state (EOS)[38]

$$P = \frac{3B_0}{2}\left[\left(\frac{V}{V_0}\right)^{-\frac{7}{3}} - \left(\frac{V}{V_0}\right)^{-\frac{5}{3}}\right]\left\{1 + \frac{3}{4}(B_0' - 4)\left[\left(\frac{V}{V_0}\right)^{-\frac{2}{3}} - 1\right]\right\}$$

where V_0 is the volume per formula unit at ambient pressure, V is the volume per formula unit at pressure P given in GPa, B_0 is the isothermal bulk modulus, and B_0' is the first pressure derivative of the bulk modulus. As a result of enough experimental data, we have set up B_0' of 4. Then, we obtained a bulk modulus of 94 ± 1 GPa. The volume V_0 is fitted to be 77.8 ± 0.2 Å^3. As is shown in Fig. 4(b), it is clearly seen that the volume of the sample at highest pressure is reduced by 20% compared with the original pressure point.

The present XRD results have confirmed that the structure *Pm*-3*m* is stable up to 49.3 GPa. Nevertheless, the recent theoretical and experimental results on another Alkaline-earth metal hexaboride CaB_6 have reported the phase transitions of CaB6 under high pressure. Most strikingly, A. N. Kolmogorov *et al*. have proposed three dynamically stable structures by a systematic analysis of multiple imaginary-frequency phonon modes when ambient structure becomes dynamically unstable around 25 GPa. The novel structure of CaB_6 was successfully quenched down to ambient pressure, which revealed a transition from ambient structure *Pm*-3*m* to tetragonal *I*4*/mmm* structure after laser-heating in DAC at 31 GPa.[19] M. Li *et al.* also found a pressure-induced phase transition at ambient temperature by means of resistance measurement and synchrotron XRD.[39] Both Ca and Ba are alkaline earth metal elements and they have the similar valence electrons $3s^2 3p^6 4s^2$ and $5s^2 5p^6 6s^2$ respectively. So we suppose that CaB_6 and BaB_6 have the same or similar propertis under pressure. We have obtained three candidate crystal structures (*I*4*/mmm*, *Cmmm*, *Cmcm*) by replacing Ca atom with Ba atom and the cell parameters, which are given in reference 19. The crystal structure prediction were also performed by CALYPSO

code[40] with two BaB_6 formula units at 100 GPa. The most stable structure is *Cmmm* which is the same structure with the replaced one. Then, we have calculated the enthalpy of the four structures mentioned above (*Pm*-3*m*, *I*4/*mmm*, *Cmmm*, *Cmcm*) by optimization method. Taking the enthalpy of *Pm*-3*m* structure as reference energy, we plotted relative enthalpy per formula unit of other three structures as a function of pressure in Fig. 5. The results illustrate that *Pm*-3*m* structure might not transform to *Cmmm* or *Cmcm* until pressure up to 78 GPa and 97 GPa respectively. The tetragonal structure (*I*4/*mmm*) discovered in CaB_6 at 31 GPa would appear in BaB_6 when pressure reaches 105 GPa. The calculation results shows that *Cmmm* have a lower enthalpy value than others after 78 GPa, so *Cmmm* structure is the most possible candidate structure. But just only by compression, ambient structure might not transform into a new structure in the same situation with CaB_6, it must be supplied some paths such as laser-heated in DAC to break the energy barrier.

It is confirmed that CaB_6 is a semiconductor with a narrow gap by means of transport measurements,[14] angle-resolved photoemission spectroscopy (ARPES) and momentum-resolved inelastic X-ray scattering.[16] Considering that the calculations with GGA-PBE would underestimate band gap, so we calculated electronic band structures with HSE06. Fig. 6 plots the band structures of BaB_6 around the Fermi level at 0 GPa and 50 GPa, which illustrates that BaB_6 is semiconductor with so narrow band gap 0.22 eV at ambient conditions. The band gap is sensitive to lattice constant *a* and wyckoff position of boron atom (0, 0, z),[4, 41] and our experimental results shows that wyckoff position (z = 0.20534) would change scarcely. So it is obvious that lattice constant decreases by compressing in Fig 3 (b) and the band gap also changes, then BaB_6 is still semiconductor with 0.34 eV at 50 GPa.

Conclusion

In this work, we have successfully investigated structural stability and compressive behaviors of BaB_6 by means of in situ high pressure synchrotron X-ray diffraction and first-principles calculations. Our experimental results reveal that it is very difficult to break the covalent network only by high pressure condition. During

experimental pressure, no phase transitions occurred and lattice constant *a* decreases linearly with pressure. Our theoretical calculations propose that the BaB6 is still semiconductor at 50 GPa. Three candidate dynamic stable structures (*Cmmm*, *Cmcm*, *I*4/*mmm*) might replace the typical cage structure at 78 GPa, 97 GPa, and 105 GPa, respectively. Attempting to accomplish the phase transition, it must be supplied some paths to break energy barrier.

Acknowledgements

The authors are grateful to Xiaodong Li and Yanchun Li for their help during the experimental research. In situ angle dispersive X-ray diffraction (ADXRD) of this work were performed at 4W2 HP-Station, Beijing Synchrotron Radiation Facility (BSRF) assistance in measurement. This work was supported by the National Basic Research Program of China (No. 2011CB808200), National Natural Science Foundation of China (Nos. 51572108, 51032001, 11504127). Program for Changjiang Scholars and Innovative Research Team in University (No. IRT1132), National Found for Fostering Talents of basic Science (No. J1103202), and China Postdoctoral Science Foundation (2015M570265).

Reference

1. P. I. Loboda, H. P. Kysla, S. M. Dub and O. P. Karasevs'ka, *Materials Science*, 2009, **45**, 108-113.
2. M. Takeda, M. Terui, N. Takahashi and N. Ueda, *Journal of Solid State Chemistry*, 2006, **179**, 2823-2826.
3. S. Kimura, T. Nanba, M. Tomikawa, S. Kunii and T. Kasuya, *Physical Review B*, 1992, **46**, 12196-12204.
4. B. Lee and L. W. Wang, *Applied Physics Letters*, 2005, **87**, 262509.
5. W. Joss, J. M. van Ruitenbeek, G. W. Crabtree, J. L. Tholence, A. P. J. van Deursen and Z. Fisk, *Physical Review Letters*, 1987, **59**, 1609-1612.
6. X. H. Ji, Q. Y. Zhang, J. Q. Xu and Y. M. Zhao, *Progress in Solid State Chemistry*, 2011, **39**, 51-69.
7. Y. Xu, L. J. Zhang, T. Cui, Y. Li, Y. Xie, W. Yu, Y. M. Ma and G. T. Zou, *Physical Review B*, 2007, **76**, 10.
8. J. M. Tarascon, J. Etourneau, P. Dordor, P. Hagenmuller, M. Kasaya and J. M. D. Coey, *Journal of Applied Physics*, 1980, **51**, 574.
9. I. Popov, N. Baadji and S. Sanvito, *Physical Review Letters*, 2012, **108**, 107205.
10. D. P. Young, D. Hall, M. E. Torelli, Z. Fisk, J. L. Sarrao, J. D. Thompson, H. R. Ott, S. B. Oseroff, R. G. Goodrich and R. Zysler, *Nature*, 1999, **397**, 412-414.
11. P. Vonlanthen, E. Felder, L. Degiorgi, H. R. Ott, D. P. Young, A. D. Bianchi and Z. Fisk, *Physical Review B*, 2000, **62**, 10076-10082.
12. J. X. Cao, Y. Zhu, Z. Q. Yang and R. Q. Wu, *Physical Review B*, 2009, **79**, 4.
13. Y. H. Han, C. X. Gao, Y. Z. Ma, H. W. Liu, Y. W. Pan, J. F. Luo, M. Li, C. Y. He, X. W. Huang and G. T. Zou, *Applied Physics Letters*, 2005, **86**, 064104.
14. B. K. Cho, J. S. Rhyee, B. H. Oh, M. H. Jung, H. C. Kim, Y. K. Yoon, J. H. Kim and T. Ekino, *Physical Review B*, 2004, **69**, 113202.
15. K. Taniguchi, T. Katsufuji, F. Sakai, H. Ueda, K. Kitazawa and H. Takagi, *Physical Review B*, 2002, **66**, 064407.
16. J. D. Denlinger, J. A. Clack, J. W. Allen, G. H. Gweon, D. M. Poirier, C. G. Olson, J. L. Sarrao, A. D. Bianchi and Z. Fisk, *Physical Review Letters*, 2002, **89**, 157601.
17. H. J. Tromp, P. van Gelderen, P. J. Kelly, G. Brocks and P. A. Bobbert, *Physical Review Letters*, 2001, **87**, 016401.
18. T. Terashima, C. Terakura, Y. Umeda, N. Kimura, H. Aoki and S. Kunii, *Journal of the Physical Society of Japan*, 2000, **69**, 2423-2426.
19. A. N. Kolmogorov, S. Shah, E. R. Margine, A. K. Kleppe and A. P. Jephcoat, *Physical Review Letters*, 2012, **109**, 075501.
20. G. H. Min, S. Q. Zheng, Z. D. Zou, H. S. Yu and H. D. Han, *Materials Letters*, 2003, **57**, 1330-1333.
21. S. Shang, T. Wang and Z.-K. Liu, *Calphad*, 2007, **31**, 286-291.
22. K. M. Schmidt, A. B. Buettner, O. A. Graeve and V. R. Vasquez, *Journal of Materials Chemistry C*, 2015, **3**, 8649-8658.
23. M. Gürsoy, M. Takeda and B. Albert, *Journal of Solid State Chemistry*, 2015, **221**, 191-195.
24. S. L. Zhou, J. X. Zhang, L. H. Bao, X. G. Yu, Q. L. Hu and D. Q. Hu, *Journal of Alloys and Compounds*, 2014, **611**, 130-134.
25. S. Massidda, R. Monnier and E. Stoll, *European Physical Journal B*, 2000, **17**, 645-649.
26. T. P. Jose, L. Sundar, L. J. Berchmans, A. Visuvasam and S. Angappan, *Journal of Mining and*

Metallurgy Section B-Metallurgy, 2009, **45**, 101-109.

27. S. Mushkolaj, J. L. Gavilano, D. Rau, H. R. Ott, A. Bianchi and Z. Fisk, *Acta Physica Polonica B*, 2003, **34**, 1537-1540.
28. H. K. Mao, P. M. Bell, J. W. Shaner and D. J. Steinberg, *Journal of Applied Physics*, 1978, **49**, 3276.
29. S. Klotz, J. C. Chervin, P. Munsch and G. Le Marchand, *Journal of Physics D-Applied Physics*, 2009, **42**, 075413.
30. A. Hammersley, S. Svensson, M. Hanfland, A. Fitch and D. Hausermann, *International Journal of High Pressure Research*, 1996, **14**, 235-248.
31. R. Young, *Oxford Science Publication*, 1993.
32. S. J. Clark, M. D. Segall, C. J. Pickard, P. J. Hasnip, M. I. Probert, K. Refson and M. C. Payne, *Zeitschrift für Kristallographie*, 2005, **220**, 567-570.
33. G. Kresse and J. Furthmüller, *Physical Review B*, 1996, **54**, 11169-11186.
34. J. P. Perdew, K. Burke and M. Ernzerhof, *Physical Review Letters*, 1996, **77**, 3865-3868.
35. A. V. Krukau, O. A. Vydrov, A. F. Izmaylov and G. E. Scuseria, *The Journal of chemical physics*, 2006, **125**, 224106.
36. J. Heyd, G. E. Scuseria and M. Ernzerhof, *The Journal of chemical physics*, 2003, **118**, 8207-8215.
37. G. Kresse and D. Joubert, *Physical Review B*, 1999, **59**, 1758-1775.
38. F. Birch, *Journal of Applied Physics*, 1938, **9**, 279-288.
39. M. Li, W. Yang, L. Li, H. Wang, S. Liang and C. Gao, *Physica B: Condensed Matter*, 2011, **406**, 59-62.
40. Y. C. Wang, J. Lv, L. Zhu and Y. M. Ma, *Computer Physics Communications*, 2012, **183**, 2063-2070.
41. S. Shah and A. N. Kolmogorov, *Physical Review B*, 2013, **88**, 014107.

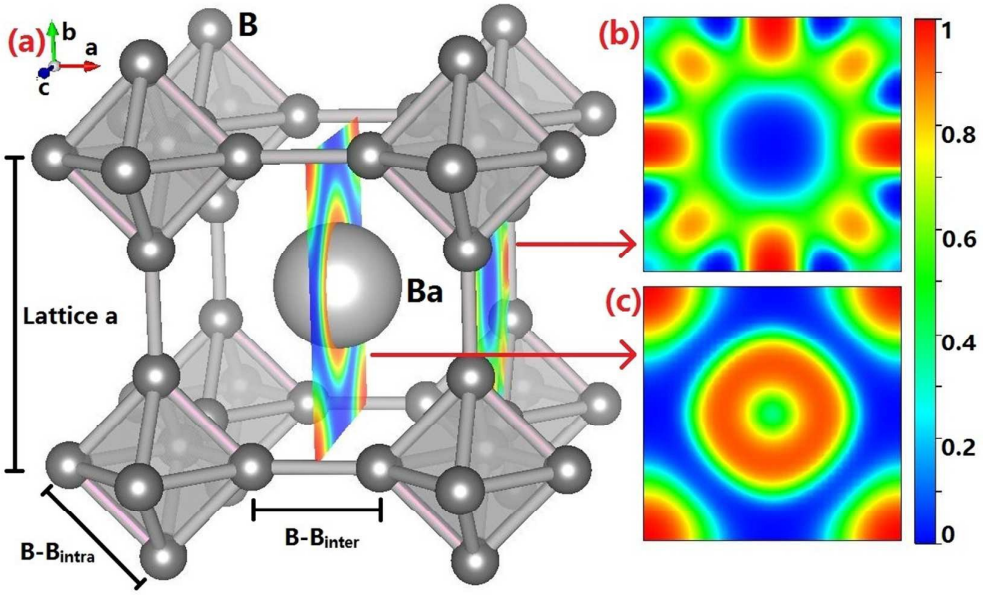

Fig. 1 (a) The *Pm*-3*m* crystal structure of BaB_6 at ambient conditions. Cubic cage formed by eight B_6 octahedrons and a central Ba cation. Octahedral surfaces shown in gray. (b) (c) Electron localization function (ELF) maps of different plan.

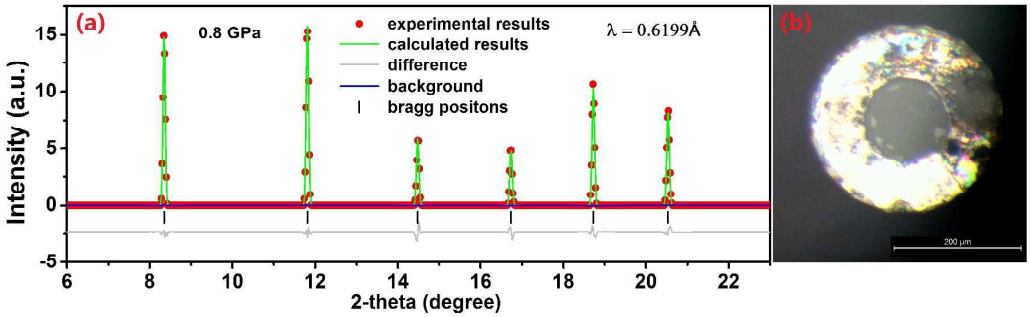

Fig. 2 (a) The Rietveld full-profile refinement of synchrotron XRD pattern at 0.8 GPa. (b) Micrograph of BaB_6 sample in DAC at 0.8 GPa just after loading pressure with PTM of methanol−ethanol−water.

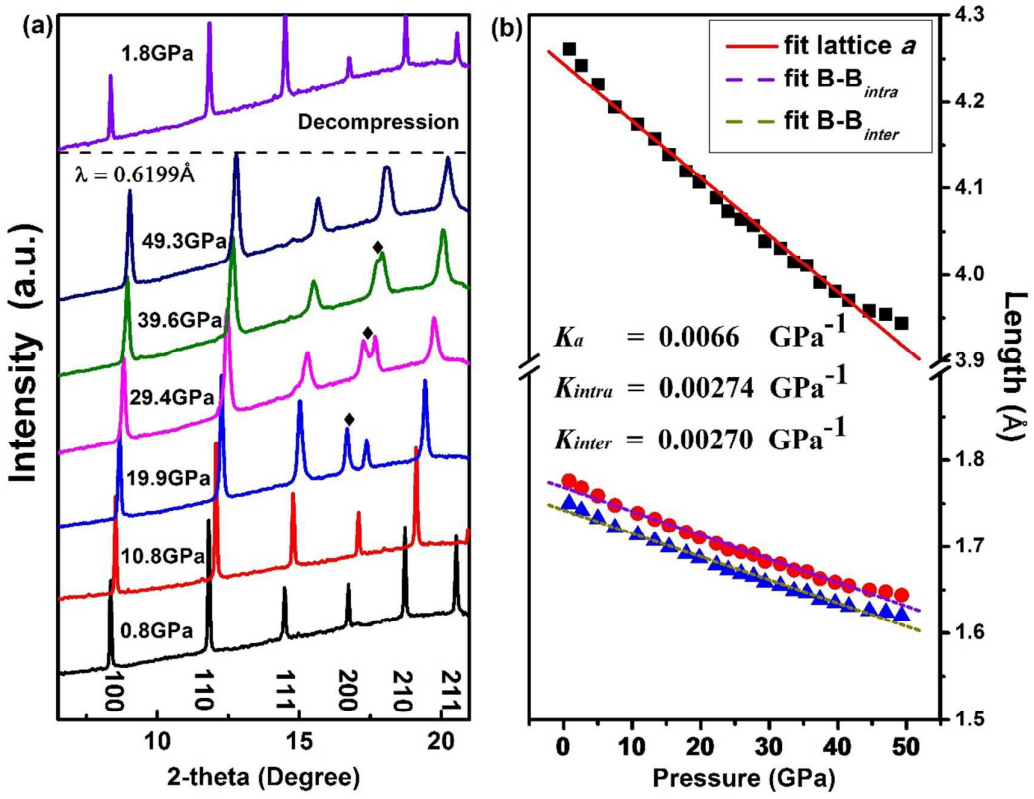

Fig. 3 (a) Typical XRD patterns at selected pressures of BaB_6 as a function of pressure on compression up to 49.3 GPa at room temperature. The peaks with marked diamonds symbols (◆) represent the bragg peaks from tungsten gasket. The wavelength of the incident X-ray beam is 0.6199 Å. (b) Evolution of the lattice constant *a* and length of B-B_{intra} bond and B-B_{inter} bond with respect to pressure. The symbols represent experimental results, and lines represent fitted results respectively.

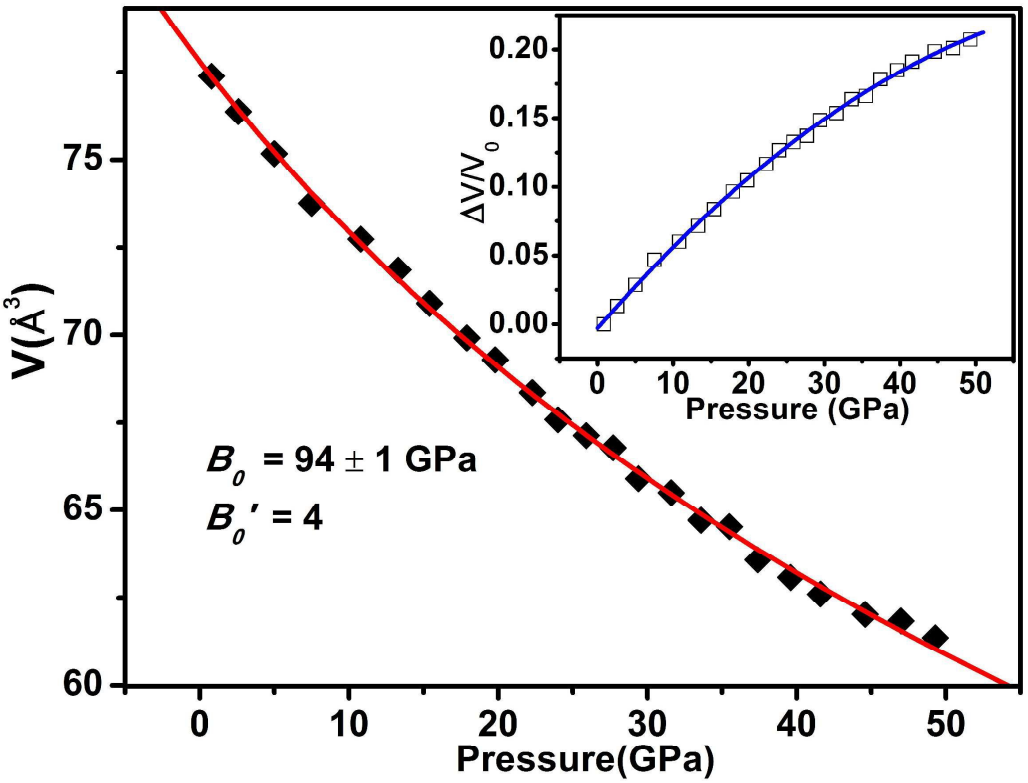

Fig. 4 (a) Pressure dependence of the unit cell volume of BaB_6. The red line shows fitted results. Insert (b) represents the volume reduction upon compressions. The blue line only shows the trend.

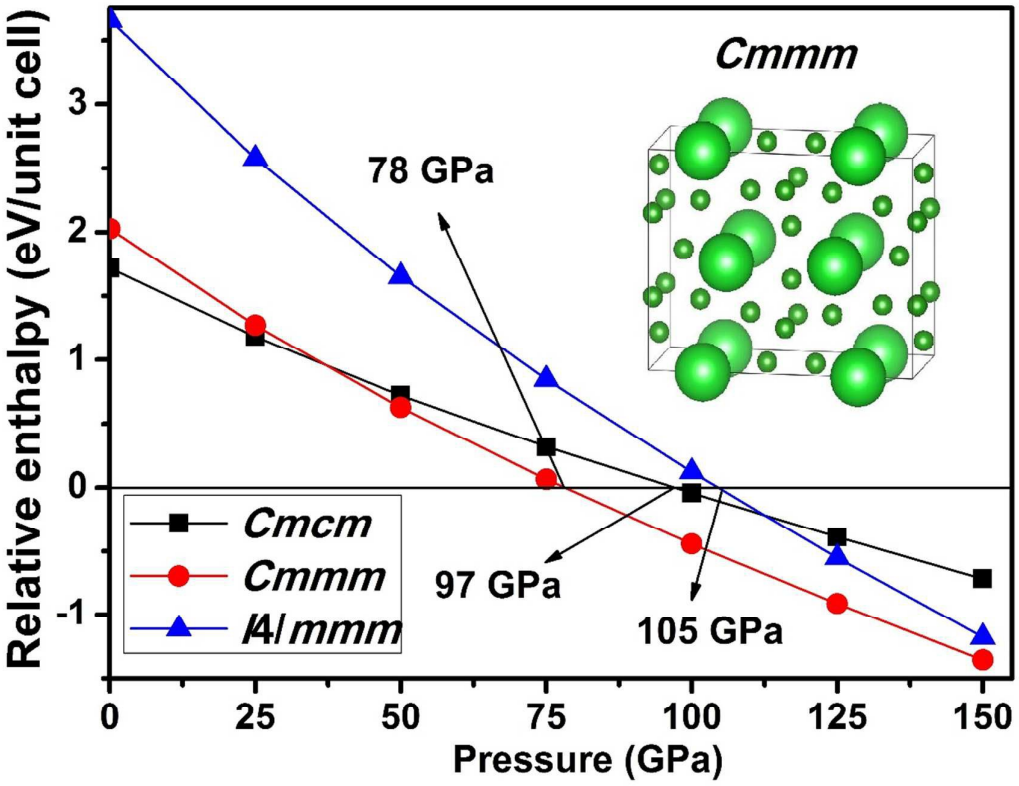

Fig. 5 The relative enthalpy per formula unit of four structures as a function of pressure for BaB_6. The enthalpy of *Pm*-3*m* structure is taken as reference energy compared with others. The inset figure represents the most possible candidate *Cmmm* structure after 78 GPa.

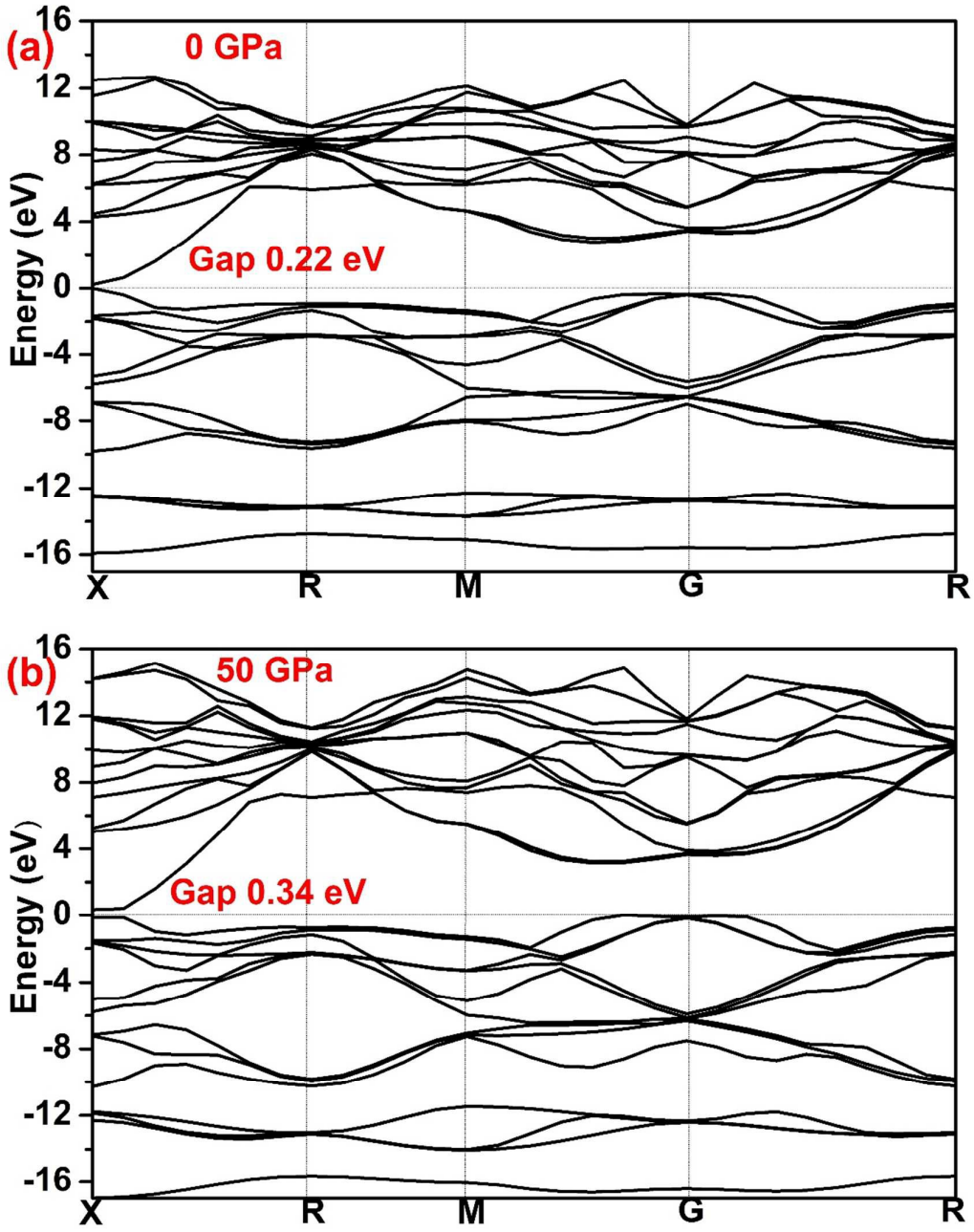

Fig. 6 Electronic band structures of *Pm*-3*m* structure (a) at 0 GPa and (b) at 50 GPa.